Response to Reviewer 1

The manuscript argues that statistical downscaling framework using machine learning can help identify convective environment for the current and future climate condition over the Arabian Peninsula. This approach is computationally less expensive than that of physics-base dynamical downscaling. The investigation is well thought. First the authors tested evaluated the performance of Random Forest, XGB, and Deep Learning. Based on the evaluation, XGB outperforms the other ML models. The investigation of convective environment is utilized the XGB model. The results exhibit a landscape of potential forecast skills of the XGB model in identifying the convective environment for the current and future climate over the Arabian Peninsula. This ML approach is promising in terms of reducing computation expenses and time. The manuscript is also well written though some figures are not clear and not easy to read and understand. Some arguments and discussion still need clarification.

We thank the reviewer for the constructive and thoughtful review, which will help us improve the clarity of figures, arguments, and discussion in the revised manuscript. Our responses are displayed in dark blue, with clickable links highlighted in contrasting dark orange.

Here are my major comments:

1. In the Introduction (line 85), you wrote "Thus, this work lays the foundation for a statistical-dynamical downscaling approach, in which CEs identified from the CMIP6 ensemble can be dynamically downscaled at convection-permitting resolution, ..." I think the study is about statistical downscaling using ML models, not dynamical downscaling.

We believe there is a misunderstanding concerning the terminology. First, we clarify the terms *downscaling*, *statistical downscaling*, *dynamical downscaling*, and *statistical-dynamical downscaling*, and then respond to the reviewer's comment.

Downscaling refers to methods used to derive regional- to local-scale climate information from large-scale model output (e.g., IPCC 2021). These methods increase the spatial resolution bridging the gap between the large-scale variables, e.g., represented by Global Climate Models (GCMs), and the smaller scales variables required for assessing regional climate change and its impacts (Maraun and Widmann 2018, p. 24).

Statistical downscaling establishes empirical relationships between large-scale atmospheric variables (predictors) and regional- to local-scale climate (predictands), whereas dynamical downscaling uses high-resolution limited-area climate models driven by boundary conditions from coarser climate model (e.g., GCM) to obtain climate information at the regional- to local-scale (IPCC 2021; Maraun and Widmann 2018; Giorgi and Gutowski 2015).

Statistical-dynamical downscaling is a hybrid approach that first uses a statistical method to identify cases or atmospheric states of interest from large-scale model output and subsequently dynamically downscale the selected cases with high-resolution regional models, as in numerous previous studies (Frey-Buness et al. 1995; Beaulant et al. 2011; Reyers et al. 2015; Meredith et al. 2018; Wang et al. 2026; Dewettinck et al. 2026).

In the present study, the ML models are used to identify CEs at 1° resolution. The ML step therefore does not itself downscale CMIP6 models. Rather, it provides a statistical case-selection framework that can subsequently be coupled with convection-permitting dynamical downscaling. Our study thus lays the foundation for such a statistical-dynamical, or case-selective, downscaling framework. To avoid ambiguity, we will reformulate the sentence in the manuscript as:

> Thus, this work lays the foundation for a statistical-dynamical (i.e., case-selective) downscaling approach, in which ML models constitute the statistical component and are employed to identify CEs in CMIP6 models; subsequently these CEs can be dynamically downscaled at convection-permitting resolution. This downscaling approach offers a computationally efficient pathway for regional climate projections over a highly sensitive and vulnerable region to climate-related hazards (Mahmoud et al., 2023; Hoteit et al., 2025).

2. It is interesting that DL and RF hardly identify the convective environment over the southern AP and the high (complex) terrain (line 260). Is it something to do with the data fed in during the training period? Or it is something related to the ML models and how they handle the data and get trained? I do not know much about ML and I think if you could explain this issue, it will be helpful for reader who would like to use ML models.

We thank the reviewer for the comment. In the revised manuscript, we will briefly discuss this issue, for example:

> The general difficulty of the ML models in classifying CEs over the southern AP and complex terrain could possibly be related to the input data and the training procedure of ML models. Firstly, since convection there is more localised and occurs at shorter timescales, predictors at 1°and 6 h resolution may poorly represent the associated atmospheric conditions. Additionally, because an instantaneous atmospheric profile is labelled based on precipitation accumulated over 6 h window, instability (e.g., CAPE) may have already been consumed by convection at the profile timestamp. Second, tree-based models outperform DL on tabular data due to various reasons such as robustness to uninformative features and ability to learn irregular functions; please refer to Grinsztajn et al. (2022) for more details. The higher XGB ability to identify CEs compared to RF may also be related to their different training procedures. In RF, multiple trees are built independently and their predictions are aggregated (i.e., bagging), whereas in XGB, trees are added sequentially with each new tree trained to improve the predictions of the existing trees (i.e., boosting). This may allow XGB to capture some of the more difficult CE patterns that are less consistently identified by RF.

3. See Figure 3. First, it will be helpful if you put note on the legend that the current, FutI and FutIII are from the CMIP6. Secondly, this sentence (line 270) "At FutI, the MM density ratio of the CE density estimate relative to the MM current one shows a slight increase up to CE probabilities of 0.7, 0.4, 0.7, and 0.5 for DJF, MAM, JJA, and SON, respectively" is not clear to where it refers in Figure 3. I think it will be better to elaborate or rephrase this sentence. Thirdly, the difference between the future CE density and that of the ERA5 (and the current) looks significant. I am aware that the future projection is from SSP5-8.5. I wonder if it is something to do with the ML model or the MM ensembles. I think it is worth

to explain or discuss in this section.

We revised the legend to "CMIP6-Current", "CMIP6-FutI", and "CMIP6-FutIII", as shown in Fig. 1 and these labels will be used throughout the revised figures. We changed the layout of Fig. 3 from 2×2 to 4×1 to improve the figure readability.

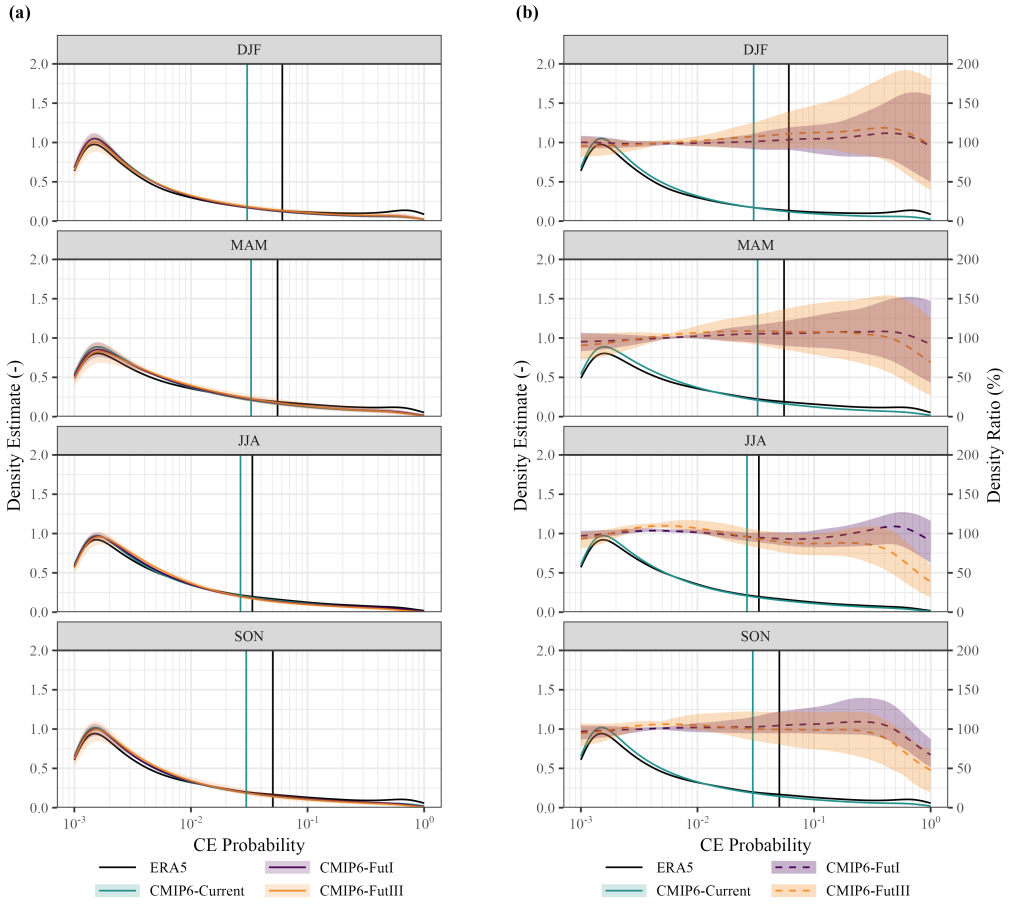


Figure 1: (a) Seasonal kernel density estimate for CE probabilities ($\geq$0.001) from XGB for ERA5 test data (solid black line) and the CMIP6 multi-model mean at the current (+1.22 °C, solid cyan line), *FutI* (+2.22 °C, solid violet line), and *FutIII* (+4.22 °C, solid orange line) regional warming levels. The vertical lines indicate the seasonal mean CE probability. The shaded areas indicate the 2.5th and 97.5th percentile range of the CMIP6 ensemble. The x-axis is $\log_{10}$ transformed.
(b) Seasonal kernel density estimate for CE probabilities ($\geq$0.001) from XGB for ERA5 test data (solid black line) and the CMIP6 multi-model mean at the current regional warming level (+1.22 °C, solid cyan line). The vertical lines indicate the seasonal mean CE probability. The right y-axis shows the density ratio of the CMIP6 multi-model mean at *FutI* (dashed violet line) and *FutIII* (dashed orange line) relative to the CMIP6 multi-model mean at the current climate regional warming level, with 100% indicates equal density. The shaded areas indicate the 2.5th and 97.5th percentile range of the CMIP6 ensemble. The x-axis is $\log_{10}$ transformed.

We will also revise the sentence near L. 273, based on the revised ML framework using absolute predictor values, to make the season-specific changes in the density ratio clearer as:

> At *FutI*, the CMIP6 multi-model density ratio relative to the current climate indicates an increase in the density over the CE-probability ranges of 0.017–0.86, 0.005–0.74, 0.21–0.77, and 0.003–0.48 for DJF, MAM, JJA, and SON, respectively. In addition, DJF and JJA exhibit additional increases over lower CE-probability ranges of 0.0010–0.0012 and 0.0018–0.014, respectively. Outside these specified ranges the CMIP6 multi-model density ratio decreases, with the largest decrease in SON (32.7%) and the smallest decrease in winter (4.55%). Noteworthy, the projected changes at *FutI* vary among individual CMIP6 models, with some models showing increases and others showing decreases in CE-probability density.

Regarding the third point, we believe there is a misunderstanding here. The original figure showed the **kernel density estimates (KDE)** only for ERA5 test data and CMIP6-Current on the left y-axis, while *FutI* and *FutIII* were shown as **density ratios (DR)** relative to CMIP6-Current on the right y-axis, for example,

$$DR_{FutI} = 100 \times \frac{KDE_{FutI}}{KDE_{Current}}$$

This was intended to avoid overcrowding the figure (Fig. 1a), and to emphasise the visualisation of the projected changes (Fig. 1b). The pronounced difference described by the reviewer is not apparent in the absolute density estimates for *CMIP6-FutI* and *CMIP6-FutIII* shown in Fig. 1a. In the revised manuscript, we will include only Fig. 1b.

4. Line 285 about Figure 4a. Over the west coast of the AP, the CE probability is quite low. In the past 20 or so years, convective events often happen in November. I wonder if the 1 deg by 1 deg grid spacing has influenced the results. Do you think the probability will get higher over the west coast of the AP if the ML model is trained with high resolution dataset?

We thank the reviewer for this question. We believe there is a misunderstanding here. The CEs probability shown in Fig. 4a represents the mean probability assigned by the ML model to atmospheric profiles with predicted CE probabilities above 0.001. Therefore, the plot describes the seasonal confidence of the ML classification not how frequently CEs occur. We agree on the point of convection occurrence during November. Enhanced CE occurrence along the west coast can be inferred from SON in Fig. 5a (first row) based on IMERG data, and XGB identifies this spatial pattern from ERA5 in Fig. 5a (second row), although with a lower frequency due to test data size (20%) of the total record.

Regarding the resolution point, a higher-resolution training dataset could potentially improve the ability of the ML model to identify localised convection, as described in our response above to comment no. 2.

5. Line 300 and Figure 5a. You wrote “Fig. 5a illustrates the seasonal climatology of CEs from IMERG, ERA5 test dataset, and MM”. I think this sentence is confusing. Isn’t the figure about the CE frequency? I also wonder why the CE frequency in ERA5 for SON is quite low over the west coast of the AP. Is it because the grid resolution is coarse (0.25 deg)?

We agree that the wording "seasonal climatology of CEs" is vague in this context and will revise it to "seasonal CE frequency".

Regarding the lower CE frequency over the west coast during SON, the seasonal CE frequency is estimated

from the ERA5 test data (as described in the figure caption) at 1° spatial resolution and 6 h intervals using XGB. Seasonal CE frequency is calculated by summing CEs within each season and year and then averaging across years. Since the test dataset contains only 20% of the samples from the total record, fewer CEs contribute to these seasonal counts, resulting in lower estimated frequencies.

6. See 325 (Bias in convective indices). You wrote, "...restricted to atmospheric profiles classified as convective by IMERG and XGB for ERA5 and CMIP6, respectively." I am not sure how IMERG can have atmospheric profile. I think it is better to reprase the sentence so that to avoid misunderstanding.

The revised sentence will read:

> Here, we assess the conditional fidelity of CMIP6 in reproducing CE components at 1°×1°in the current climate by comparing atmospheric profiles from ERA5 that are labelled as CEs based on precipitation from IMERG against atmospheric profiles from CMIP6 that are classified as CEs by XGB.

7. Line 350 Figure 8 and S10. What do you think is the reason of colder and drier theta-e in the CMIP6 models? Is it something to do with model error calculation? Or something to do with the ML model training?

We thank the reviewer for raising this point. The negative θ_e biases in CEs from CMIP6 models compared to ERA5 are not an isolated feature and are consistent with the negative PW, T_{d2m}, and MUCAPE biases.

To identify the origin of the negative θ_e bias in the CMIP6 models compared to ERA5, we compared the joint probability density of air temperature at 2 m (T_{a2m}) and dew-point temperature at 2 m (T_{d2m}) from the CMIP6 models with ERA5, as shown in Fig. 2. First, we considered all atmospheric profiles regardless of whether they were classified/labelled as CEs or not (left column). The joint-density differences occur mainly along the T_{d2m} axis, indicating a general tendency towards reduced near-surface moisture rather than substantial differences in T_{a2m} (Fig. 2; left column). Therefore, the negative near-surface θ_e bias appears to originate primarily from bias in CMIP6, and it is unlikely to originate from the ML classification. This conclusion is also supported by Fig. 3, where PW, and T_{d2m} are generally negatively biased.

Second, CMIP6 models show an underestimation of CEs near the saturation boundary compared to ERA5 (Fig. 2; right column), while the compensating density shifts are model dependent and reflect varying combinations of temperature and moisture differences. These results indicate that the negative moisture biases persist within the CE subset, although their relative temperature and moisture contributions become model dependent. This is why we recommended further evaluation of CMIP6 models using radiosonde observations at L. 446 to better pinpoint the origin of these biases. Nevertheless, we will add this diagnostic and discussion to the revised manuscript.

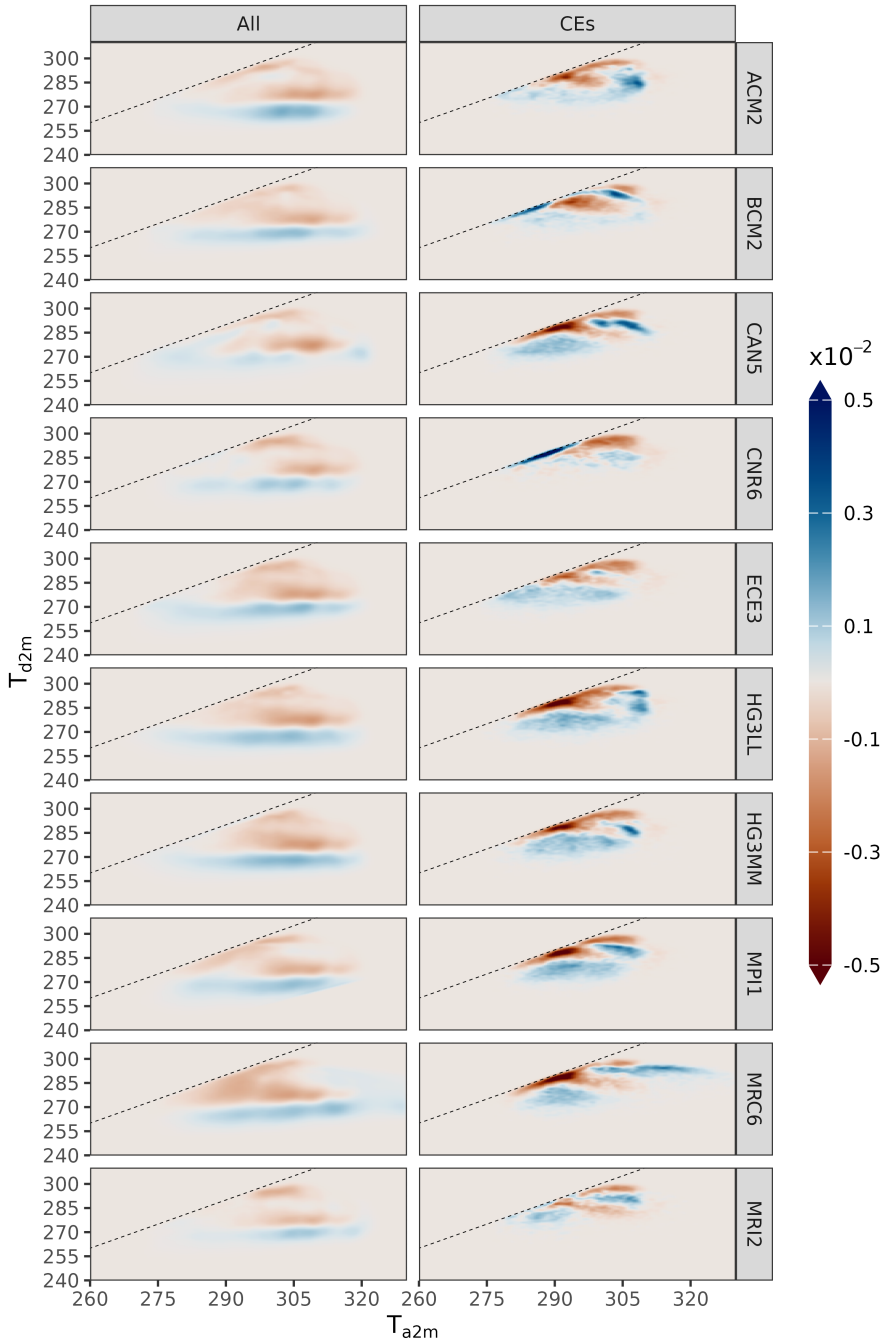


Figure 2: Difference in the bivariate probability density of near-surface air temperature (T_{a2m}) and dew-point temperature T_{d2m} for each model (rows) relative to ERA5, for all atmospheric profiles (CEs and non-CEs; left column) and only CE profiles (right column). The dashed diagonal line indicates the saturation boundary (RH $\approx$ 100%).

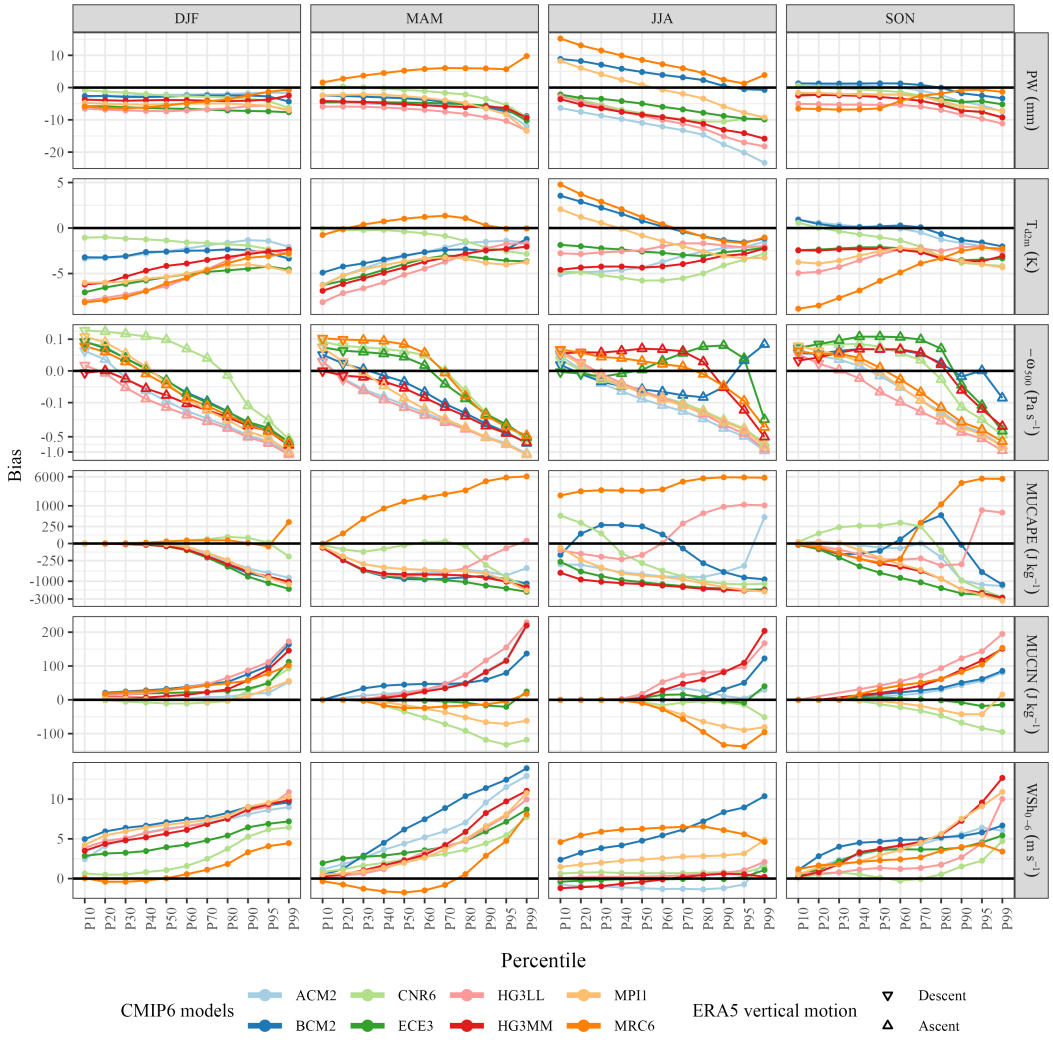


Figure 3: Seasonal biases at different percentiles for precipitable water (PW; first row), 2 m dew-point temperature (Td_{2m}; second row), negative vertical velocity at 500 hPa ($-\omega_{500}$; third row), most unstable CAPE (MUCAPE; fourth row), most unstable CIN (MUCIN; fifth row), and 0–6 km wind shear ($WSh_{0\text{-}6}$; sixth row) in CEs from CMIP6 models at the current regional warming level relative to ERA5. The axes for MUCAPE and ω_{500} are pseudo-log transformed with sigma values of 100 and 0.025, respectively. Triangles in the ω_{500} panels indicate whether the corresponding ERA5 percentile represents descent or ascent. CMIP6 models are shown as solid lines with point markers: ACM2 (light blue), BCM2 (blue), CNR6 (light green), ECE3 (green), HG3LL (light pink), HG3MM (red), MPI1 (light orange), and MRC6 (orange). The horizontal black line indicates zero bias.

8. Line 415 (Discussion). How can we apply this XGB model for short-term forecasts? Will the coarse grid spacing (> 1.0 deg) helps identify convective events (e.g., rain)? Or you need to train the XGB with higher resolution dataset?

We thank the reviewer for these questions. In this study, XGB does not forecast the atmospheric state itself but uses information about the atmospheric state to classify it as a CE or non-CE. As we mentioned in line L. 529, XGB can be applied to ECMWF HRES or IFS forecasts, and depending on the results, for instance, spatially widespread high probabilities of CEs, a dynamical downscaling or forecast can be

performed. This approach in an operational setting can reduce computational resources.

We would advise using higher spatiotemporal resolution in such an operational setting. Our preliminary experiments showed that higher spatiotemporal resolution can improve CE identification. At the beginning of this project, we trained an RF model using hourly atmospheric profiles at 0.25°resolution and obtained POD, 1 - FAR, and HSS values above 0.7. However, for the present study, we needed to degrade the spatial and temporal resolution of the IMERG-ERA5 data to avoid the mismatch with CMIP6 data. One should also consider in an operational setting whether, for example, ECMWF provides all variables needed by the trained XGB model here; otherwise, retraining would be warranted.

9. Line 425. It is a nice note to acknowledge the likelihood of having poor representation with 1 deg resolution. I wonder why not you considered MERGIR brightness temperature as one of the variables in the ML training. The brightness temperature can easily indicate the development (life cycle) of convection based on the cloud top temperature. The colder it gets, the more severe the convection is. Precipitation may happen (or may not), and yet updraft and horizontal winds may also happen during the lifetime of the convective clouds. Do you think the results of your study would change if you included the MERGIR brightness temperature dataset?

We thank the reviewer for the valuable suggestion. Infrared brightness temperature could potentially improve the classification skill of the ML models. However, the choice of predictors in the present study is constrained by their availability in CMIP6 archive, since the ML models are subsequently applied to CMIP6 data. Although outgoing longwave radiation (OLR) can be converted to an infrared brightness temperature (e.g., Yang and Slingo 2001; Feng et al. 2023), subdaily OLR output is not consistently available across CMIP6 models. For example, for SSP future scenarios, OLR at a subdaily temporal resolution is available from only a few modelling groups (https://esgf-metagrid.cloud.dkrz.de/search?project=CMIP6&activeFacets=%7B%22activity_id%22%3A%22ScenarioMIP%22%2C%22variable_id%22%3A%22rlut%22%2C%22frequency%22%3A%5B%22subhrPt%22%2C%223hr%22%5D%7D).

10. Summary and conclusions. I see that the variables for training in this study are mostly short-memory variables, i.e., change within hours or days. I have a dumb question. Will long-memory variable such as SST or soil moisture would affect the ML model, and so the results of this study, given that the data training is over seasonal and annual scales? In my humble opinion, the training would affect the models. The model may learn the atmospheric dynamics in a longer scale too.

We thank the reviewer for the interesting questions and comments. Indeed, long-memory variables such as SST and soil moisture can influence convection through ocean–atmosphere (e.g., Al-Mutairi et al. 2019; Tuel et al. 2022; Khan et al. 2026) and land-atmosphere interactions (e.g., Lee and Hohenegger 2024; Liu et al. 2022). However, part of this influence might be already included in the dynamic and thermodynamics variables used to train the ML models. Explicitly identifying the spatial and temporal-lag structure of these long-memory variables would require a dedicated analysis and is beyond the scope of the present study.

Nevertheless, we performed a brief exploratory analysis of the relationship between southern Red Sea SST and CE occurrence. First, CEs were summed at each grid point over three fixed periods within each calendar month: days 1–10, 11–20, and 21 to the end of the month, giving 36 periods per year. Second,

Global OSTIA SST data (Worsfold et al. 2024) were used to estimate the mean SST over the southern Red Sea (36° E–44° E, 13° N–20° N) for the same periods; then, climatological annual cycle was removed to obtain SST anomalies (SST'). Finally, the relationship between CE sum and SST anomalies was examined at lags of 0, 10, 20, and 30 days using a negative-binomial regression (Venables and Ripley 2002) fitted independently at each grid point as

$$\log(\mu_{x,y,t}) = \alpha_{x,y} + \beta_{x,y}^{(L)} SST'_{t-L} + \gamma_p, \tag{1}$$

where $\mu_{x,y,t}$ is the expected CE sum, $\alpha_{x,y}$ is the intercept, $\beta_{x,y}^{(L)}$ is the SST anomaly coefficient for lag L, and γ_p represents the seasonal cycle ($p = 1, \ldots, 36$). The rate ratio ($RR = e^{\beta}$) is the multiplicative change in the expected CE sum for a +1 K SST anomaly.

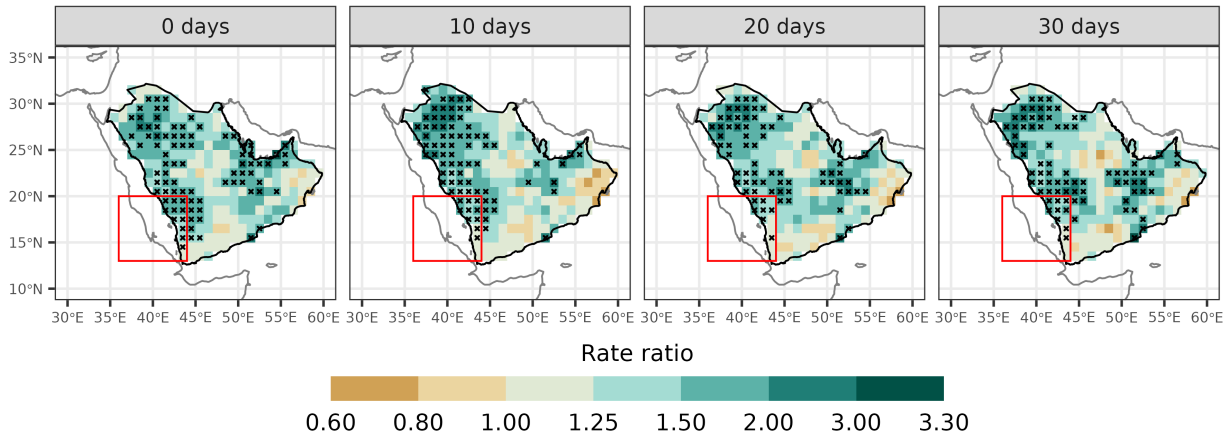


Figure 4: Rate ratio of CE occurrence associated with +1 K southern Red Sea SST anomaly at lags of 0, 10, 20, and 30 days. An increase in the expected CE sum with warmer SST anomalies is associated with RR greater than one and is shown in green, while a decrease is associated with RR less than one and is shown in brown. Stippling indicates grid points where the SST coefficient is statistically significant at $p < 0.05$. The red box indicates the considered southern Red Sea region. The colour scale is log_e transformed.

At the considered lags, the northwestern and western AP show a significant positive relationship with southern Red Sea SST anomalies ($p < 0.05$), while the southeastern region shows either an insignificant positive relationship or a negative relationship (Fig. 4). These exploratory results suggest that the influence of SST is spatially heterogeneous and temporally variable and deserves a dedicated study. In the revised manuscript, we will highlight the influence of SST and soil moisture as a direction for future work and that ML models could possibly benefit from such variables.

Here are my minor comments:

1. In the Abstract and Introduction, you wrote that "remains computationally prohibitive" (line 1 and 80, respectively). I do not think it is prohibitive. Computational resources in big institutions like KAUST or NCAR could do a large ensemble hi-res simulation. I think it is computationally expensive, not prohibitive.

We will replace "computationally prohibitive" to "computationally expensive" in both instances in the revised manuscript.

2. See Table 2. It will be helpful to spell out what FutI and FutIII are in the caption. Also, it will be helpful to explain a bit what each of them is in the text.

The new caption for Table 2 will read:

> Time periods corresponding to three regional warming levels from CMIP6 models. Current denotes +1.22 °C regional warming above the preindustrial level and includes historical simulations only; FutI and FutIII denote future regional warming levels of +2.22 °C and +4.22 °C above the preindustrial level, respectively, and are based on the SSP5-8.5 scenario.

We will also revise the sentence in L128 to:

> In addition, we analysed two periods from the SSP5-8.5 scenario corresponding to an additional +1 °C (*FutI*) and +3 °C (*FutIII*) of regional warming relative to the current level, equivalent to regional warming levels of +2.22 °C and +4.22 °C above preindustrial levels, respectively.

3. Figure 7. It will be helpful to add title for each row in the figure. The first row is PW, second row is Td, third row is w, and so on.

Figure 7 will be replaced with Fig. 3.

4. Figure 9a. Please confirm which axis is MUCIN and which one is MUCAPE.

Thanks for pointing out this typo. The y-axis represents MUCIN and the x-axis represents MUCAPE. The typo will be corrected in the revised manuscript.

References

Beaulant, A-L. et al. (2011). "Statistico-dynamical Downscaling for Mediterranean Heavy Precipitation". In: *Quarterly Journal of the Royal Meteorological Society* 137.656, pp. 736–748. ISSN: 0035-9009, 1477-870X. DOI: 10.1002/qj.796.

Dewettinck, Wout et al. (2026). "Case-Selective Dynamical Downscaling Enables a Tenfold Cost Reduction for Extreme Precipitation Statistics". In: *Geophysical Research Letters* 53.9, e2026GL122330. ISSN: 1944-8007. DOI: 10.1029/2026GL122330.

Feng, Zhe et al. (2023). "Mesoscale Convective Systems in DYAMOND Global Convection-Permitting Simulations". In: *Geophysical Research Letters* 50.4, e2022GL102603. ISSN: 1944-8007. DOI: 10.1029/2022GL102603.

Frey-Buness, F., D. Heimann, and R. Sausen (1995). "A Statistical-Dynamical Downscaling Procedure for Global Climate Simulations". In: *Theoretical and Applied Climatology* 50.3-4, pp. 117–131. ISSN: 0177-798X, 1434-4483. DOI: 10.1007/BF00866111.

Giorgi, Filippo and William J. Gutowski (2015). "Regional Dynamical Downscaling and the CORDEX Initiative". In: *Annual Review of Environment and Resources* 40.1, pp. 467–490. ISSN: 1543-5938, 1545-2050. DOI: 10.1146/annurev-environ-102014-021217.

Grinsztajn, Léo, Edouard Oyallon, and Gaël Varoquaux (2022). "Why Do Tree-Based Models Still Outperform Deep Learning on Typical Tabular Data?" In: *Proceedings of the 36th International Conference on Neural Information Processing Systems*. Nips '22. Red Hook, NY, USA: Curran Associates Inc. ISBN: 978-1-7138-7108-8.

IPCC (2021). "Annex VII: Glossary [Matthews, J.B.R. and Möller, V. and van Diemen, R. and Fuglestvedt, J.S. and Masson-Delmotte, V. and Méndez, C. and Semenov, S. and Reisinger, A. (Eds.)]" In: *Climate Change 2021: The Physical Science Basis. Contribution of Working Group I to the Sixth Assessment Report of the Intergovernmental Panel on Climate Change*. Ed. by V. Masson-Delmotte et al. Cambridge, United Kingdom and New York, NY, USA: Cambridge University Press, pp. 2215–2256. DOI: 10.1017/9781009157896.022.

Khan, Basit et al. (2026). "On the Role of Sea Surface Temperature in the 16 April 2024 Rainstorm Over the United Arab Emirates". In: *Geophysical Research Letters* 53.3, e2025GL118215. ISSN: 1944-8007. DOI: 10.1029/2025GL118215.

Lee, Junhong and Cathy Hohenegger (2024). "Weaker Land–Atmosphere Coupling in Global Storm-Resolving Simulation". In: *Proceedings of the National Academy of Sciences* 121.12, e2314265121. DOI: 10.1073/pnas.2314265121.

Liu, Weicheng et al. (2022). "The Influence of Soil Moisture on Convective Activity: A Review". In: *Theoretical and Applied Climatology* 149.1, pp. 221–232. ISSN: 1434-4483. DOI: 10.1007/s00704-022-04046-z.

Maraun, Douglas and Martin Widmann (2018). *Statistical Downscaling and Bias Correction for Climate Research*. 1st ed. Cambridge: Cambridge University Press. ISBN: 978-1-107-06605-2. DOI: 10.1017/9781107588783.

Meredith, Edmund P., Henning W. Rust, and Uwe Ulbrich (2018). "A Classification Algorithm for Selective Dynamical Downscaling of Precipitation Extremes". In: *Hydrology and Earth System Sciences* 22.8, pp. 4183–4200. ISSN: 1607-7938. DOI: 10.5194/hess-22-4183-2018.

Al-Mutairi, Motirh et al. (2019). "On the Effect of Red Sea and Topography on Rainfall over Saudi Arabia: Case Study". In: *Atmosphere* 10.11, p. 669. ISSN: 2073-4433. DOI: 10.3390/atmos10110669.

Reyers, Mark, Joaquim G. Pinto, and Julia Moemken (2015). "Statistical–Dynamical Downscaling for Wind Energy Potentials: Evaluation and Applications to Decadal Hindcasts and Climate Change Projections". In: *International Journal of Climatology* 35.2, pp. 229–244. ISSN: 1097-0088. DOI: 10.1002/joc.3975.

Tuel, Alexandre et al. (2022). "Extreme Storms in Southwest Asia (Northern Arabian Peninsula) under Current and Future Climates". In: *Climate Dynamics* 58.5, pp. 1509–1524. ISSN: 1432-0894. DOI: 10.1007/s00382-021-05975-7.

Venables, W. N. and B. D. Ripley (2002). *Modern Applied Statistics with S*. Fourth. ISBN 0-387-95457-0. New York: Springer.

Wang, Songning et al. (2026). "Future Climate Projections of Hazardous Convective Weather Using an Ensemble of Environment-informed, Convection-permitting Dynamical Downscaling Simulations". In: (). DOI: 10.1029/2025JD045354.

Worsfold, Mark et al. (2024). “Presenting a Long-Term, Reprocessed Dataset of Global Sea Surface Temperature Produced Using the OSTIA System”. In: *Remote Sensing* 16.18. ISSN: 2072-4292. DOI: 10.3390/rs16183358.

Yang, Gui-Ying and Julia Slingo (2001). “The Diurnal Cycle in the Tropics”. In: *Monthly Weather Review* 129.4, pp. 784–801. ISSN: 1520-0493, 0027-0644. DOI: 10.1175/1520-0493(2001)129<0784:TDCITT>2.0.CO;2.